

Petrographical and geochemical constraints on the origin of the igneous intrusions in Gilgit Metamorphic Complex, northern Kohistan Island Arc (Pakistan): Implications for Petrogenesis, magma evolution and tectonic setting

Masroor Alam^{1*}, Hasnain Ali², Iqtidar Hussain³, Zahid Hussain⁴, Muhammad Azam¹, Sher Sultan Baig⁵, Javed Akhtar Qureshi⁵, and Hawas Khan⁵

¹Department of Earth Science China University of Geosciences Beijing PR China

²Department of Earth Sciences Lanzhou University, PR China

³Department of Earth Sciences Central South University Changsha, PR China

⁴College of Oceanography, Hohai University, Nanjing 210098, PR China

⁵Department of Earth Science, Karakorum International University, Gilgit Baltistan, Pakistan

*Corresponding author: masroor.alam@kiu.edu.pk

Submitted date: 27/04/2020 Accepted date: 08/03/2024 Published online: 31/03/2024

Abstract

The small granitic and volcanic intrusions in the Gilgit Metamorphic Complex in the northern Kohistan Island Arc are not studied till date. As a result, the petrogenesis, magma evolution and tectonic setting of these igneous intrusion are conjectural. In this contribution, we present petrography, major and trace elements data of these igneous intrusion from Sakar Koi to Chimis Dass area Gilgit with a view to describe their petrogenesis, magma evolution and geodynamic setting. The rocks mainly contain quartz, plagioclase, biotite, muscovite, olivine, pyroxene, biotite, and hornblende with some accessory minerals such as apatite, sphene and zircon. The SiO₂ and Na₂O+K₂O values are in range of 53.60 to 73.19 wt.% and 4.55 to 9.129 wt.%, respectively. Geochemically, the rocks were recognized as granite, granodiorite, and gabbroic-diorite and basalt trachy andesite based on TAS diagrams for plutonic and volcanic rocks. The values of A/NK and A/CNK are in the range of 1.32 to 3.14 Wt.% and 0.67 to 1.50 wt. %, respectively indicating calc-alkaline metaluminous magma series except granite rock which is peraluminous. In tectonic discrimination diagram, the granite and granodiorite fall in the syn-collisional field and the gabbroic-diorite show volcanic arc environment. According to the ratios of k/Rb (112.54-970 wt.%) and Ba/Rb (0.1-2.9 wt.%), the granite and granodiorite were highly evolved, while the gabbro-diorite and basalt trachy andesite which show higher values of Fe₂O₃ (112.54 wt.% and 8.13 wt.%, respectively) and MgO 6.56 and 5.76 wt.%, respectively) with higher ratios of K/Rb (970 and 924.86 wt.%, respectively) and Ba/Rb (8.3 and 2.9 wt.%, respectively) indicating that these rocks were comparatively less evolved. Field observation, available geochemical and petrographic data indicate the source for rocks is upper mantle and magmatism was more acidic with time and formed granite and granodiorite.

Keywords: Fractionation; geochemistry; petrography; Syn-collision; Kohistan Island Arc.

1. Introduction

Development of the Kohistan Island Arc took place as a result of northward movement of neo-Tethyan oceanic crust and subduction underneath the Asian Plate in early cretaceous to late Jurassic period (Bard et al., 1979; Jadoon et al., 2021; Zafar et al., 2020). After an intense work done by various researchers, Kohistan now has been divided into six main lithologies from south to north: the Jijal mafic-ultramafic complex (Petterson, 2010), Kamila amphibolites (Jan and Tahirkheli, 1979), the Chilas Complex (Jan, 1970; 1977), Dir-Utror

volcanic (Tahirkheli and Jan, 1979; Jan, 1979), the Kohistan batholiths (Patterson and Windley, 1985; Zhang et al., 2021), the Chalt volcanics (Tahirkheli and Jan, 1979), and the Yasin Group of sediment (Tahirkheli and Jan, 1979; Pudsey et al., 1985; Pudsey, 1986).

Kohistan batholith extends 270 km east-west and 50-60 km north south and is part of Trans-Himalayan batholiths which extends some 2700 km towards east (Ali et al., 2021). The Kohistan batholith comprises various types of lithologies from hornblendite to leucogranites especially gabbro, gabbroic

diorite and granite in composition (Petterson, 2010). In Kohistan batholith, intrusion is horizontally and vertically with significant dimension. Small intrusions were also emplaced in the form of sill and dykes and other geometrical shapes. The common minerals in the Kohistan batholith intrusion are plagioclase, alkali feldspar, hornblende, biotite and quartz (Petterson, 2010). Based on Rb-Sr whole rock isochron ages (Patterson and Windley, 1985) divided the batholith as 102 ± 12 Ma for an early, deformed, tonalite, 54 ± 4 Ma and 40 ± 6 Ma for two second stage granitoids, and 34 ± 14 Ma and 29 ± 8 Ma for late leucogranitic sheets. The first researcher (Pudsey, 1986) near Shandur Pass in Shamaran area identified volcanic rocks and was given the name Shamaran volcanics and described that the northern margin of the Kohistan batholiths and Shamaran volcanic were intruded by acidic plutons of the Kohistan Batholith. Kohistan represented Andean type magmatism in three places, the Utror volcanic, the un-deformed part of Kohistan batholith and Shamaran/Teru volcanics (Petterson, 2010, Ali et al., 2021). Early researchers have focused on the Kohistan Batholith and Chalt/Shamaran volcanic along Hunza and Ghizer River in the northern Kohistan Island Arc, but the intrusions in the Gilgit metamorphic complex were previously not studied. Therefore, our study focuses on the small magmatic and volcanic intrusions of Kohistan batholith and Shamaran Volcanics, respectively, which are intruded in the Gilgit metamorphic complex near Gilgit town. Our study area is limited 10 to 9 km along the road from Chilmis Das to Sakarkoi area where these intrusions are well exposed (Fig. 2).

In this study, petrography and geochemistry were conducted on these intrusions with the aim of discussing petrogenesis, classification, and constraining the tectonic setting under which these rocks were intruded. Our study aims to fill the existing research gap on these intrusions in the Gilgit Metamorphic Complex in the northern part of the Kohistan Island arc.

2. Geological setup of the study area

Geographically, the Kohistan Island Arc is located within in the northern Area of Pakistan

and tectonically bounded between MMT (Main Mantel Thrust) and MKT (Main Karakoram Thrust) (Jadoon et al., 2021; Ali et al., 2021). There are other Neo-Tethyan ophiolites outcropped in the North of Pakistan such as Dargai Complex ophiolite (Ullah et al, 2020; Ullah et al., 2022) and Sapat complex (Ullah et al., 2023). But Kohistan Island Arc comprises mantle to uppermost crust lithologies and shows complete section in the world, the only comparable section to Kohistan is Jurassic Talkeentna terrain in Alaska (Petterson, 2010). Development of the Kohistan Island Arc took place as a result of northward movement of Neo-Tethyan oceanic crust and subduction underneath the Asian Plate in early cretaceous to late Jurassic times (Shah and Shervais, 1999; Jadoon et al., 2021; Ali et al., 2021). The Nanga Parbat Haramosh Massif split the Kohistan-Laddakh Arc along the border of Kohistan with Baltistan area (Petterson, 2010). In the Kohistan Island Arc Andean margin phase found in three places; 1) the Dir-Utror volcanics which contain theolitic to calc-alkaline lavas and composed of 53% basalt and 79% rhyolite, 2) the Kohistan batholith which is part of Trans Himalayan batholith and intruded during intra-oceanic phase, and 3) the Teru/Shamaran volcanics. Petterson (2010) summarized all the work and described all key lithostratigraphy which includes the entire geology from the south to north. The Kohistan Island Arc is subdivided into six various units which include Jijal complex, Kamila amphibolite, Chilas complex, metaplutonic belt, the Juglote and Dir-Utror groups, and Yasin group (Dhuime et al., 2009) shown in figure 1. In the southern part of the Kohistan Island Arc the Kamila amphibolite is extending across the east-west (Petterson, 2010). The Kamila amphibolites mostly consist of mafic rock suits, but they also contain ultramafic, granitic, diorite plutons and rare sediments (Bignold et al., 2006). In the Kohistan and Swat area these amphibolites are found in two belts. The amphibolites forming the southern belt are the products of petrograd metamorphism and are basic to intermediate in nature and intruded into tufts, but tufts are now banded amphibolites. Amphibolites in granulite belt show retrograde metamorphism, which is due to influx of water and product of pyroxene granulite (Tahirkheli and Jan, 1979).

The Jijal complex contains metamorphosed mafic to ultramafic rocks but these rocks contain original igneous texture, layering of minerals and cumulus (Dhuime et al., 2009; Petterson, 2010). Along the Indus River between Patten and Jijal areas, this complex is well exposed (Petterson, 2010). The Jijal complex mostly consists of lower dunnites, websterites, harburgites, pyroxenite, and upper garnet granulites (Dhuime et al., 2009).

The Chilas complex extends 300 km E-W with a width of 40 km. Most of the rocks in the complex are calc-alkaline intrusive rocks ranging from mafic to ultramafic in composition (Bignold et al., 2006). The Chilas complex is dominated by diorites and gabbro-norites while other rocks are present in subordinate proportion which includes gabbros, mafic dykes, troctolites, peridotite, anorthosite, and dunnites (Khan, 1994; Ali et

al., 2021). In northern Pakistan, the Kohistan batholith is bounded by northern and southern suture zones and it belongs to trans-Himalayan batholith which extends eastward as Ladakh batholith in the northwest India and extends as a Gangdese batholith in southern Tibet (Patterson and Windley, 1985). The Kohistan batholith is largely intrusive into the Chalt volcanics and Juglote group of rocks (Bard et al., 1979; Jadoon et al., 2021; Ali et al., 2021). The Kohistan batholith evolved in three main stages; first the plutonic stage (110-90 Ma) which is represented by foliated gabbro-diorites and Matum Das tonalite (Jadoon et al., 2021). In the second stages between (85-40 Ma) the undeformed gabbro, granite and diorite are intruded by general mafic to acid rocks (Jadoon et al., 2021). The third stage emplaces leucogranite and granite sheets intruded at 30 Ma which are mainly formed of biotite, muscovite and garnet (Jadoon et al., 2021).

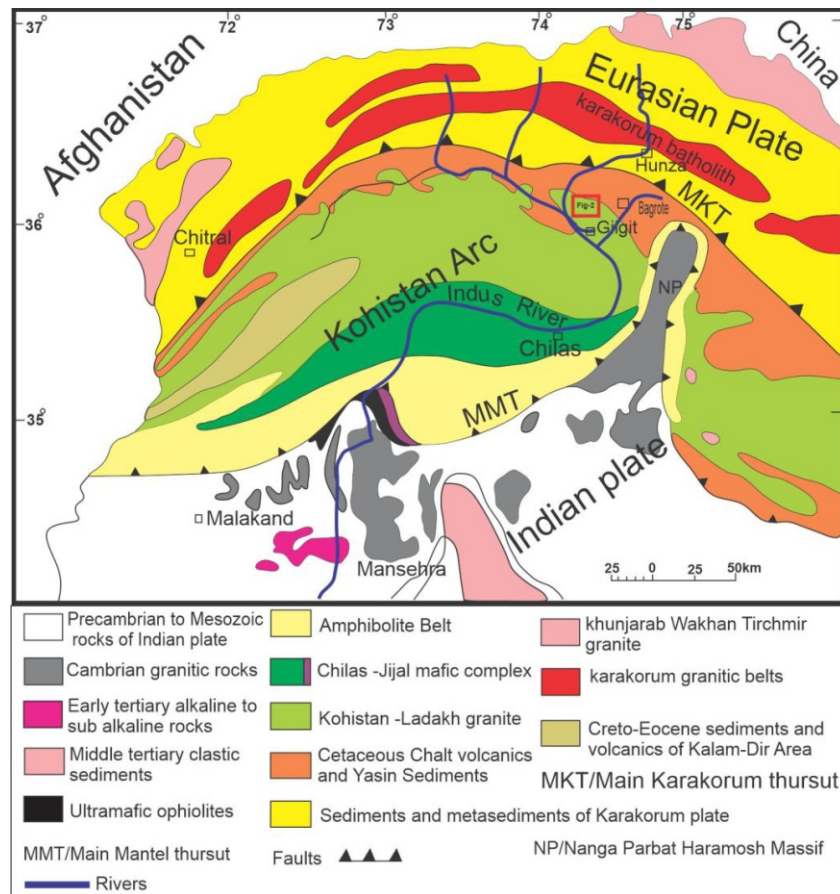


Fig. 1. General geologic map of the Kohistan-Ladakh terrane (modified after Searle et al, 1996; Sharma, 1991).

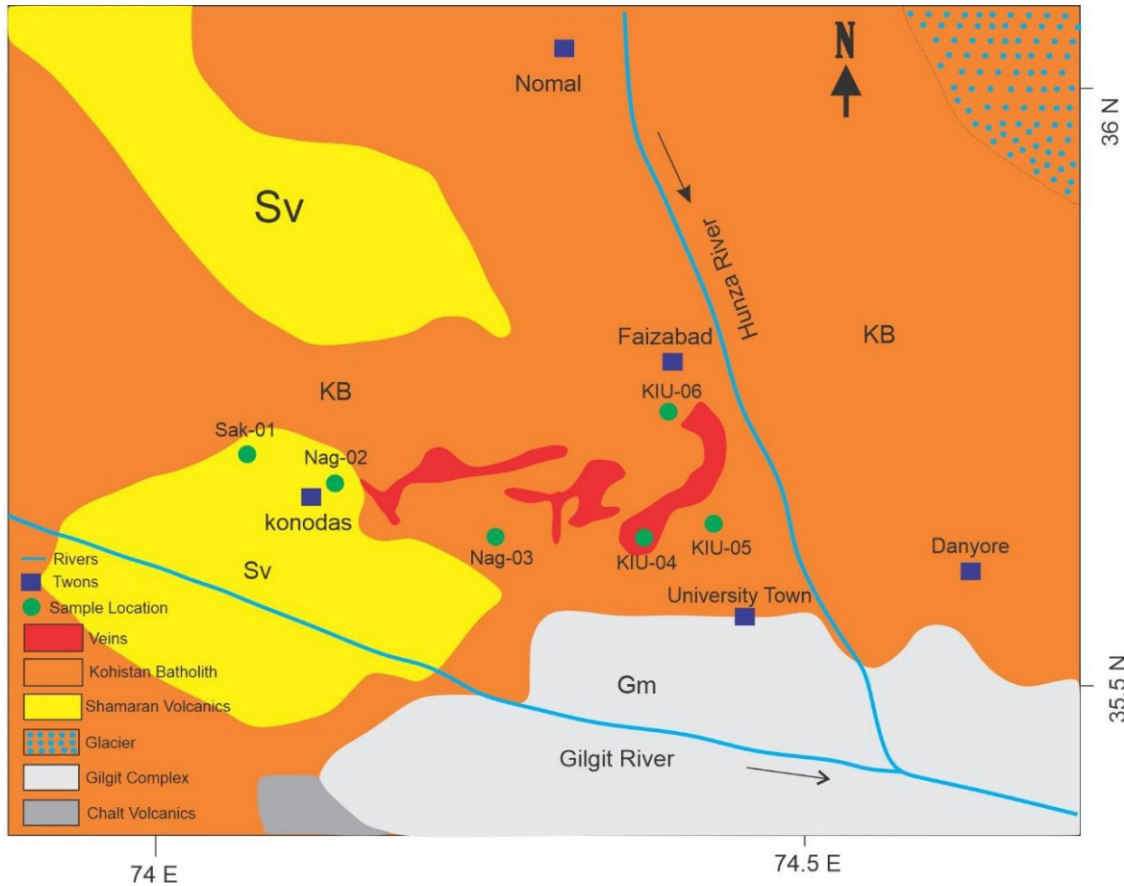


Fig. 2. Shows the map of study area, modified after Searle et al. (1996).

3. Sampling and analytical techniques

A total of 6 fresh/less altered samples were collected from different intrusions in the study area. These samples were carried at National Centre of Excellence in Geology (NCEG), University of Peshawar for thin section and XRF studies. For the thin section, first samples were cut down by a rock cutting machine into small slabs then these slabs were grounded by using carbide powder from 600 grit. Then the samples were put on the hot plate at 80 °C for 24 hours to dry and then mounted on the slab and glass slide by using epoxy. Final stage was to polish the slides by using 1000 grit carbide powder to prepare thin sections. Five samples were analyzed at the National center of Excellency Geology Peshawar for major and trace elements by X-Ray fluorescence spectrometry (WDXRF) using standard techniques.

4. Results

4.1 Petrography

The dominant minerals in gabbroic-diorite rock (Fig. 3) of the study area are plagioclase, biotite, quartz, hornblende, apatite, and sphene. Chlorite exists as a secondary mineral. The gabbroic diorite is medium grained rock containing anhedral to subhedral plagioclase with albite and Carlsbad twinning and it shows sharp boundaries with other associated minerals. Quartz is anhedral and shows scatter characteristics and also contains pleochroic halos. Greenish chlorite is also observed and might be formed as the result of chloritization of muscovite. The rock shows poikilitic texture under the petrographic microscope in which the biotite grain host quartz grain as inclusion. Biotite flakes contain rims of hornblende. Biotite also contains pleochroic halos and it exists as a primary mineral. Quartz form anhedral to subhedral crystals with wavy extinction (Fig. 3).

The granite rock (Fig. 4) is medium grained, inequigranular rock containing quartz

and K-feldspar as dominant minerals. K-Feldspar shows microperthite texture containing albite lamellae. Quartz in the rock is as anhedral form and is bordered by muscovite and biotite. Plagioclase exists as subhedral

shape and showing sharp boundaries with other minerals. The rocks also contain sillimanite mineral. Biotite shows well developed boundaries with other minerals. Zircon and apatite are found as accessory minerals.

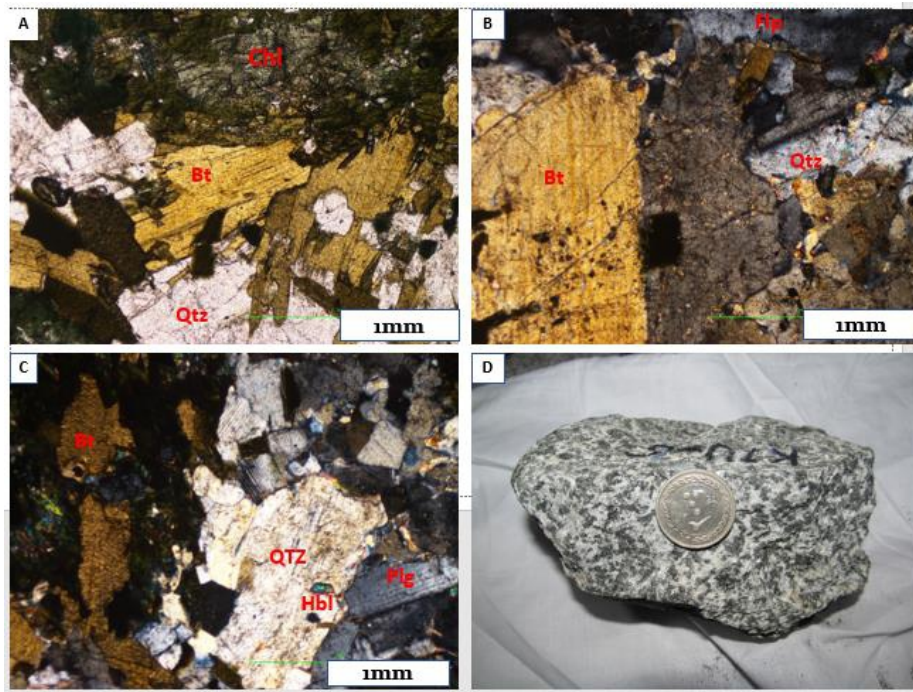


Fig. 3. Photomicrographs show the investigated petrographic features in gabbroic-diorite rock of study area: a) chloritization of muscovite, and also biotite, and anhedral quartz with wavy extension, b) brownish biotite and feldspar, c) subhedral quartz contain hornblende in between and plagioclase with twinning, and d) hand specimen of the gabbroic diorite.

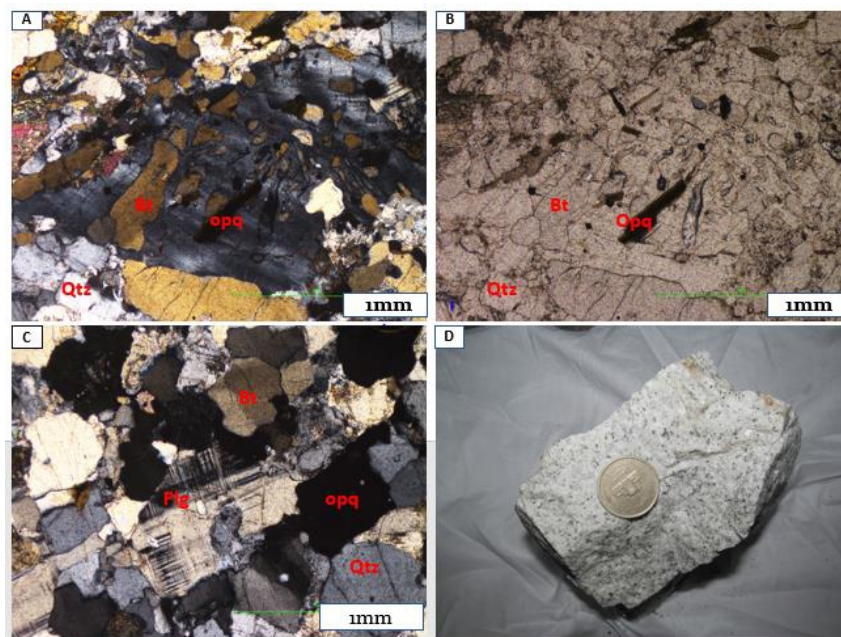


Fig. 4. Photomicrographs show the investigated petrographic features in granite rock of study area: a, b) are in XPL and PPL, respectively, show anhedral quartz, biotite and opaque, c) shows subhedral plagioclase feldspar, and d) hand specimen of the granite rock.

The medium grained granodiorite rock is composed mainly of quartz, plagioclase, k-feldspar, muscovite, hornblende and biotite. Quartz contains the inclusion of hornblende and exists as anhedral form. The rock contains primary and secondary biotite which contains pleochroic halos. Hornblende contains biotite and quartz grain. Apatite and zircon are the

accessory minerals in the rock (Figs. 5-6). The volcanic rock which is recognized as basalt trachy andesite shows fine grained texture under petrographic microscope, quartz shows anhedral crystal habit. The brownish biotite shows distinct cleavage, while feldspar shows subhedral habit, distinct cleavage with normal extinction.

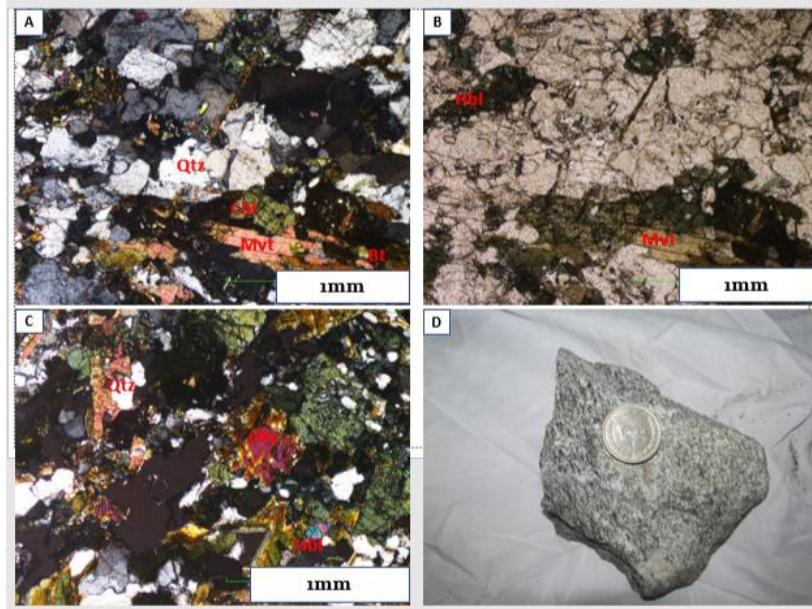


Fig. 5. Photomicrographs show the investigated petrographic features in the granodiorite rock of study area: a, b) are in XPL and PPL, respectively, containing anhedral quartz grain with undulose extinction, chlorite, brownish biotite, and muscovite with subhedral form, c) olivine, hornblende, and Quartz. and d) hand specimen of the granodiorite.

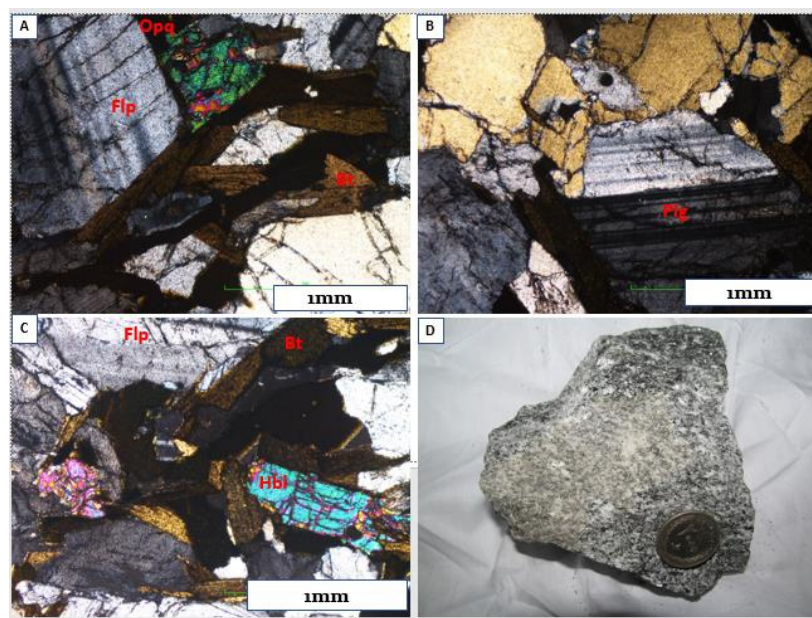


Fig. 6. a) Subhedral feldspar grains with twinning, opaque and brownish biotite with perfect cleavage, b) subhedral grains of plagioclase with Carlsbad albite polysynthetic twinning, c) feldspar, biotite, and subhedral hornblende grain, and d) hand specimen of granodiorite.

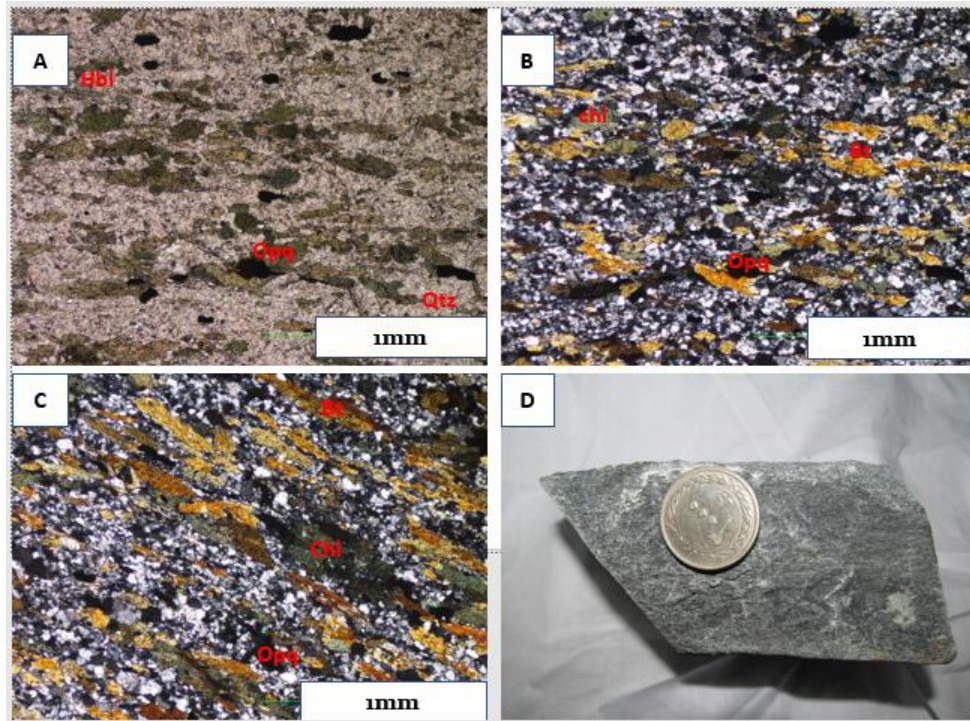


Fig. 7. Photomicrograph of the volcanic rock from the study area: a, b) are in PPL and XPL respectively, showing anhedral greyish quartz, opaque hematite, and subhedral hornblende show pleochroism in PPL, c) Chlorite, biotite and opaque minerals, and d) Basalt trachy andesite.

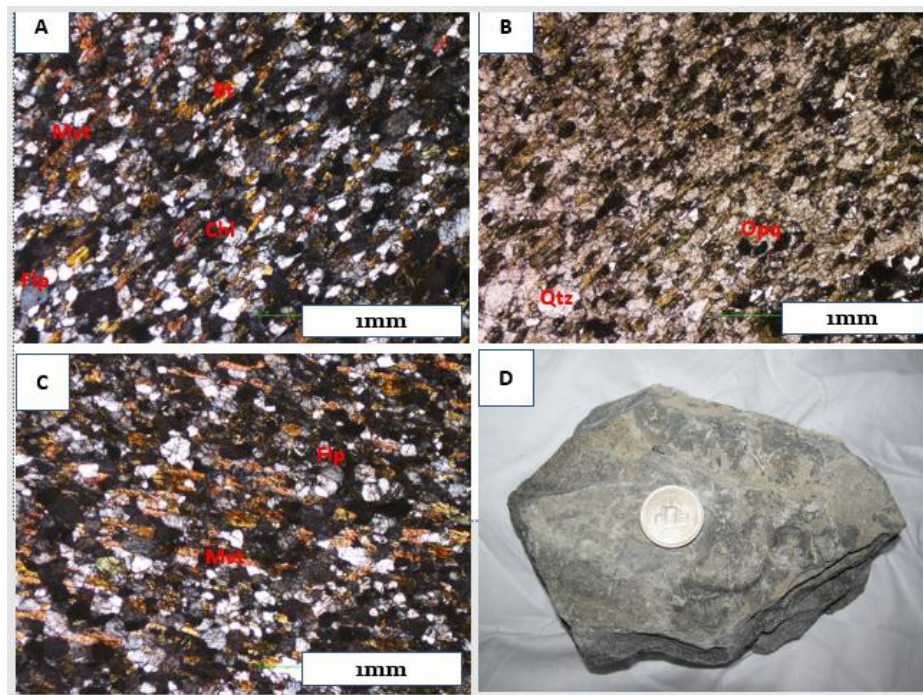


Fig. 8. Photomicrographs and hand specimen of the volcanic rock: a, b) are in both in XPL and PPL, whitish quartz anhedral in in XPL, brownish biotite with cleavage and normal extension, greenish chlorite and hornblende with low interference color.

The muscovite, greenish chlorite, and hornblende show low interference colors. Hornblende, Muscovite and Feldspar crystals show subhedral habit. The microphotographs of the volcanic rock both in PPL and XPL are shown in the (Figs. 7-8). The subhedral habit, distinct cleavage with normal extinction characteristics are obvious. The muscovite, greenish chlorite and hornblende show low interference colors. Hornblende, Muscovite and Feldspar crystals show subhedral habit.

4.2 Whole rock geochemistry

4.2.1 Major elements

The geochemistry analytical results are shown in Table 1. The major elements such as SiO₂, TiO₂, Al₂O₃, Fe₂O₃(t), MnO, MgO, CaO, Na₂O, K₂O, and P₂O₅ were analyzed (Table 1). The highest content of SiO₂ was observed in granite which is 73.19 wt%, while it was lowest in concentration (53.60 wt%) in gabbroic diorite. The content of TiO₂ ranges from 0.11 wt.% to 0.95 wt.% and the highest content is found in basalt trachy andesite. Al₂O₃ content ranges from 15.445 wt.% in granite to 17.15 wt.% in gabbroic diorite. In addition, Fe₂O₃(t) is highest, i.e., 10.03 wt.% in gabbroic diorite while it is lowest in concentration in granites of the study area. While medium to high concentrations such as, 5.23 and 8.13 wt.% were analyzed in granodiorite and basalt trachy andesite respectively. The contents of MnO and P₂O₅ are lowest in studied rocks ranging from 0.08 wt.% to 0.27 wt.% and 0.04 wt.% to 0.24 wt.%, respectively. The value of Na₂O+K₂O is highest in granite which is 9.13 wt.% while it is lowest in gabbroic diorite (4.55 wt.%). The Rb/Sr values of the studied samples range from 0.04 to 2 wt% which is highest in the granite and lowest in gabbroic diorite. While the other rock suits such as granodiorite and basalt trachy andesite show Rb/Sr value of 0.7 and 0.4 wt%, respectively. In addition, the values of A/NK and A/CNK are in the range of 1.32 to 3.14 wt.% and 0.67 to 1.50 wt%, respectively. The A/NK value is highest in granodiorite and lowest in granite. While the A/CNK value is highest in granite and lowest in basalt trachy andesite (Table 1)

4.2.2 Trace elements

The trace element, i.e., Ti, Cr, Rb, Sr, Zr, Ni, V, Zn, Cu, Ba, and K are analyzed using XRF technique and shown in Table 1. Ti and K elements are abundant, ranging from 2190 ppm to 14310 ppm and 29100 ppm to 138730 ppm with a mean value of 10512 ppm and 72302 ppm, respectively. The content of Ni ranges from 130 ppm to 300 ppm with an average value of 198 ppm, while Y and V concentration shows medium values, ranging from 30 ppm to 130 ppm and 480 ppm to 850 ppm with an average of 75 ppm and 710 ppm, respectively. The elements Y, V, and Zn are below detection limits in the granite samples as shown in Table 1.

5. Discussion

5.1 Petrogenesis

The granitoids are classified by using TAS diagram of Cox (2013). In the classification diagram, the granitoid rocks fall in the field of gabbro-diorite, granodiorite and granite, while the volcanic rocks fall in the field of basalt trachy andesite in the TAS diagram of LeBase et al. (1986) (Fig. 9 and 12).

In AFM ternary diagram (Fig. 13), the granitoids show calc-alkaline geochemical signature. To discriminate magma series, i.e., metaluminous, peraluminous and peralkaline, the ternary diagram A/CNK verses A/NK (Fig. 11) was used and the rocks fall in the range of metaluminous except granite which shows peraluminous signature. The SiO₂ content of the gabbro diorite is comparatively lower (53wt%) while that of granodiorite and granite is intermediate (63-65%) and high (73%) respectively (Table 1). The SiO₂ verses major element variation diagram (Fig. 14) shows linear trend for granite and granodiorite relative to basalt trachy andesite and gabbroic-diorite.

In addition, with the increasing content of SiO₂, decreasing concentration of MgO and Fe₂O₃ are observed, and the enrichment of Na₂O and K₂O in melt shows evolution in the magma by crystal fractionation for both granite and granodiorite. All the samples of granitoids contain higher content of K₂O than Na₂O which indicates fractionation in different magma pulses (Jung and Hoernes, 2000). The

relatively constant values of K_2O/Na_2O or $K_2O > Na_2O$ indicate similar magma sources (Jung and Hoernes, 2000). On the other hand, the major elements of the gabbro-diorite and basalt trachy andesite show different trends with the decreasing content of SiO_2 and increasing percentage of MgO and Fe_2O_3 , which reflect limited evolution of the rocks with respect to granite and granodiorite. The volcanic rock which contains 54% SiO_2 and falls in the range

of basalt trachy andesite field, is enriched in K_2O (8%), Fe_2O_3 , MgO and with low Na_2O (0.8%). The gradual increase of Na_2O+K_2O from intermediate to acidic with the increase of SiO_2 is shown in figure 10. The granite and granodiorite cross cut both basalt trachy andesite and gabbroic-diorite or diorite, and enriched in Na_2O+K_2O from intermediate to acidic rocks, due to magmatism more acidic with time (and Windley 1985).

Table. 1. Major and trace elements concentration of igneous intrusion of the study area. Major elements are in wt% and trace elements are in ppm.

Rock type	Grano diorite	Granite	Gabbro -diorite	Granodi orite	Basalt-trachy andesite
Sample	Nag2	Kiu4	kiu5	kiu6	Nag3
SiO2	63.22	73.187	53.60	65.09	54.588
TiO2	0.913	0.113	0.817	0.781	0.951
Al2O3	16.35	15.445	17.14	16.04	15.781
Fe2O3(5.715	0.878	10.02	5.232	8.128
MnO	0.078	0.027	0.273	0.103	0.106
MgO	1.534	0.172	6.563	1.133	5.763
CaO	5.343	1.428	7.259	6.415	7.231
Na2O	2.984	3.331	1.032	2.782	0.847
K2O	3.035	5.798	3.518	3.08	6.231
P2O5	0.132	0.041	0.243	0.213	0.131
Total	99.18	100.379	100.2	100.6	99.626
Na2O+	6.019	9.129	4.55	5.862	7.078
Na2O/	0.98	0.57	0.29	0.9	0.85
K/Rb	130.8	112.54	970	180.8	924.86
Rb/Sr	0.7	2.00	0.04	0.7	0.4
Ba/Rb	0.2	0.1	8.3	0.4	2.9
A/NK	3.14	1.32	1.82	1.85	1.72
A/CNK	0.86	1.50	0.87	0.81	0.67
Trace elements in ppm					
Ti	14310	2190	1153	1167	12860
Cr	950	980	750	1110	510
Rb	450	700	30	310	150
Sr	650	350	700	450	400
Zr	1100	280	b.d.l	350	110
Ni	240	130	190	300	130
Y	30	b.d.l	90	50	130
V	670	b.d.l	840	480	850
Zn	300	b.d.l	370	240	140
Cu	460	330	630	360	510
Ba	109	92	250	130	321
K	58860	78780	2910	5604	138730

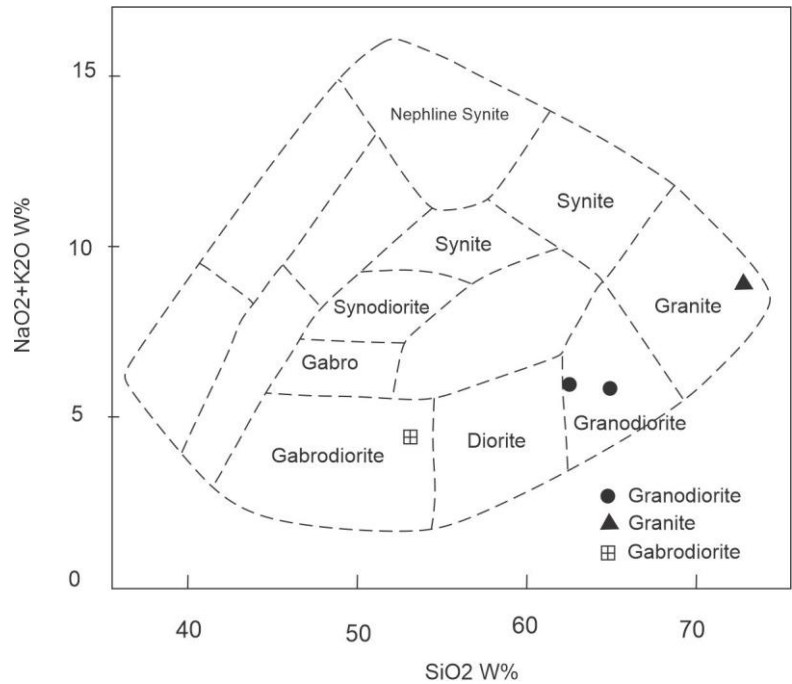


Fig. 9. TAS diagram of Cox (2013) shows the classification of plutonic rocks of study area.

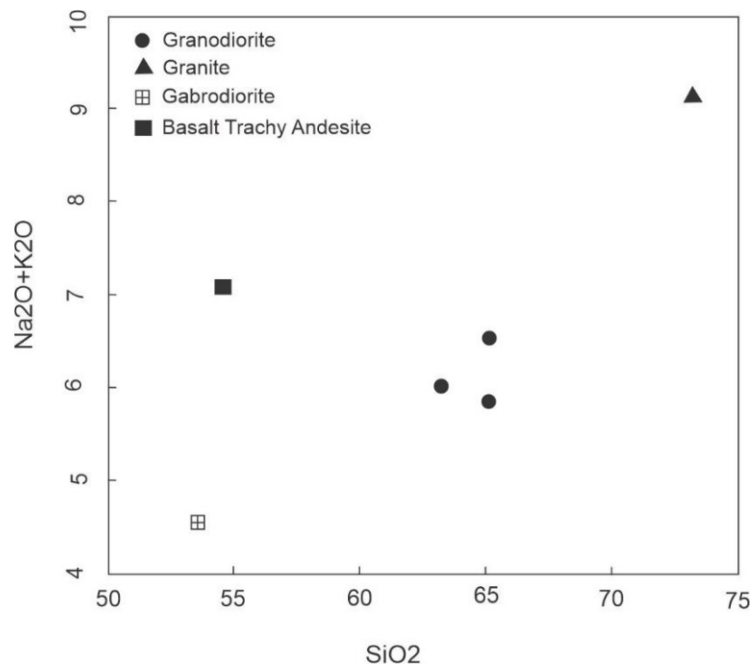


Fig. 10. Shows the increasing trend of Na₂O+K₂O from gabbroic-diorite, basalt trachy andesite, and granodiorite to granite when plotted against SiO₂.

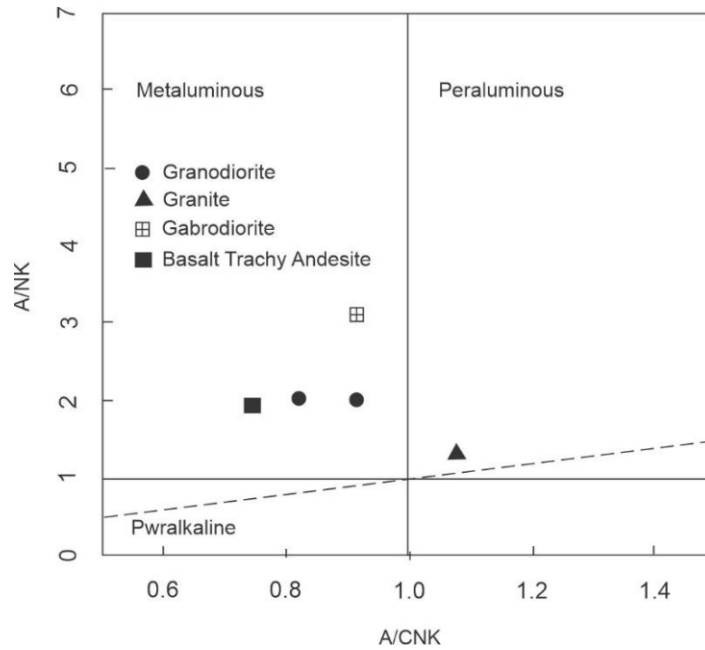


Fig. 11. A/CNK versus A/NK diagram of Shand (1943) for granitoid in which all granitoid fall in the field of peraluminous except granite, see text for discussion.

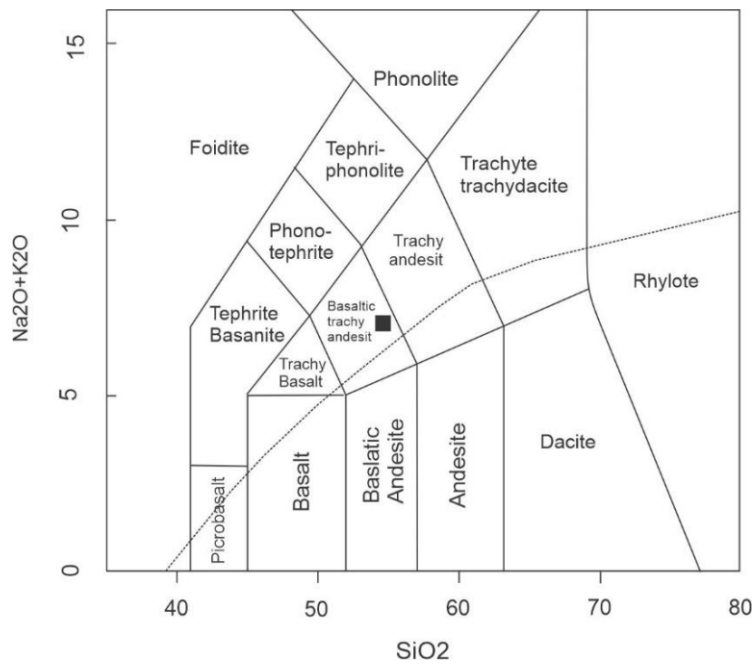


Fig. 12. TAS diagram shows the classification of volcanic rocks of study area. Modified from Le Bas et al. (1986). See text for discussion.

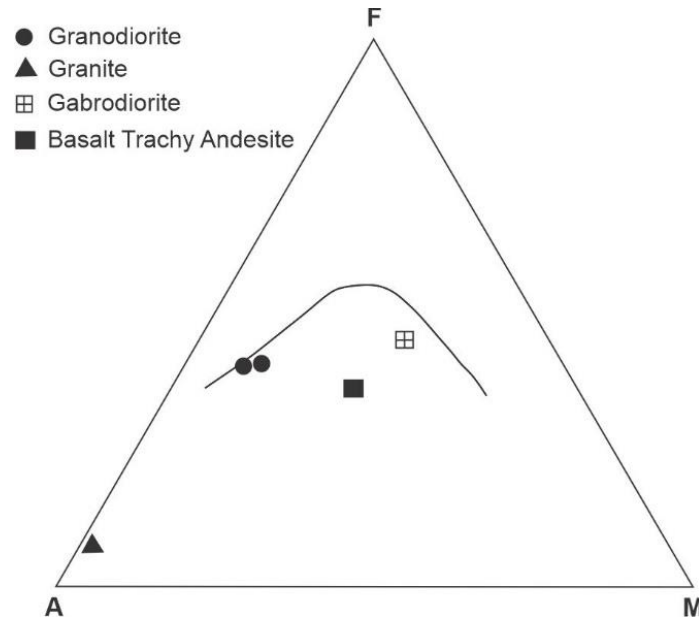


Fig. 13. AFM diagram shows the magma series trend for rocks of study area, all sample show calc- alkaline trend. Modified from Irvine and Baragar (1971), see text for discussion.

4.3 Magma evolution and geodynamic setting

The trace elements data are presented in Table 1, and the variation diagrams for the trace element versus SiO_2 are shown in the Figure 15. The concentration of large ion lithophile elements Rb, K and Ba increases with increasing SiO_2 in the granite and granodiorite with respect to the HFSE. In granodiorite, HFS elements such as Zr and V also show enrichment. The enrichment of HFS elements (Zr and V) is due to the considerable concentration of volatiles during magma evolution (Ugbe et al., 2016). Generally, in granite and granodiorite the K and Rb act incompatibly, but in the gabbroic diorite or diorite and basalt trachy andesite, both show variation from LILE element to HSF elements. The LILE elements (Rb and Ba) show low values with respect to the HFSE (V and Zr). The Y content decreases with increasing SiO_2 in all samples of the studied granitoids with respect to the other trace element. The gradual decrease of Y with increasing SiO_2 shows hornblende and pyroxene fractionation because Y is highly compatible with both (Lee, 1997).

The elemental ratios such as K/Rb, Sr/Rb and Ba/Rb are determined and listed in the

Table 1 and are plotted against SiO_2 in the Figure 15. According to Blevin (2004), K/Rb ratio is a useful indicator for magma fractionation because both K and Rb are mantle incompatible, as both K and Rb have large ionic radius, hence can't be substituted in the same site, as a result both retain in the residual melt. The granite and Granodiorite rocks show values of $\text{K/Rb} < 200$ and $\text{Ba/Rb} < 0.4$ and show strong fractionation trends. On the other hand, the gabbroic diorite and basalt trachy andesite are less evolved as the $\text{K/Rb} > 200$ and also $\text{Ba/Rb} > 1$ with obscured fractionation trend. The gabbroic diorite shows Rb/Sr ratio below average (0.25). Field observation, geochemical and petrographic data reveal that the source for these rocks was upper mantle and magmatism was more acidic with time, i.e., from granite to granodiorite crystallization (Pettersson, 2010). In addition, the tectonic discrimination diagrams of Pearce et al. (1984) (Fig. 17), the granite and granodiorite fall in syn-collisional field and the gabbroic diorite and basalt trachy andesite show volcanic arc environment, indicating that the granitoids are emplaced during collision of Kohistan with India or Karakorum while the basalt trachy andesite formed in the intra oceanic arc before collision.

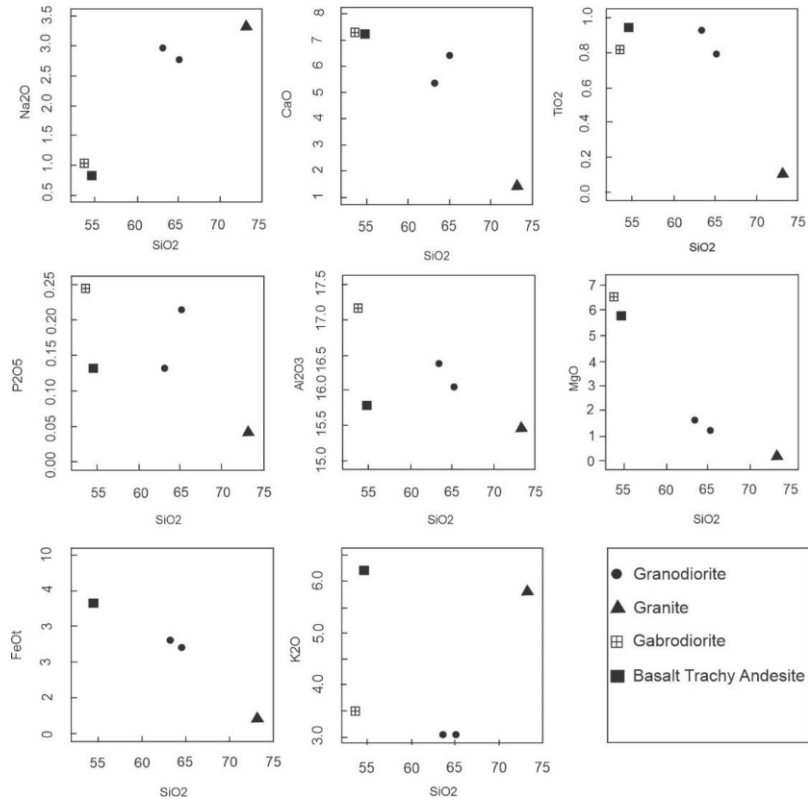


Fig. 14. Harker type variation diagram for major elements of the rocks, see text for discussion.

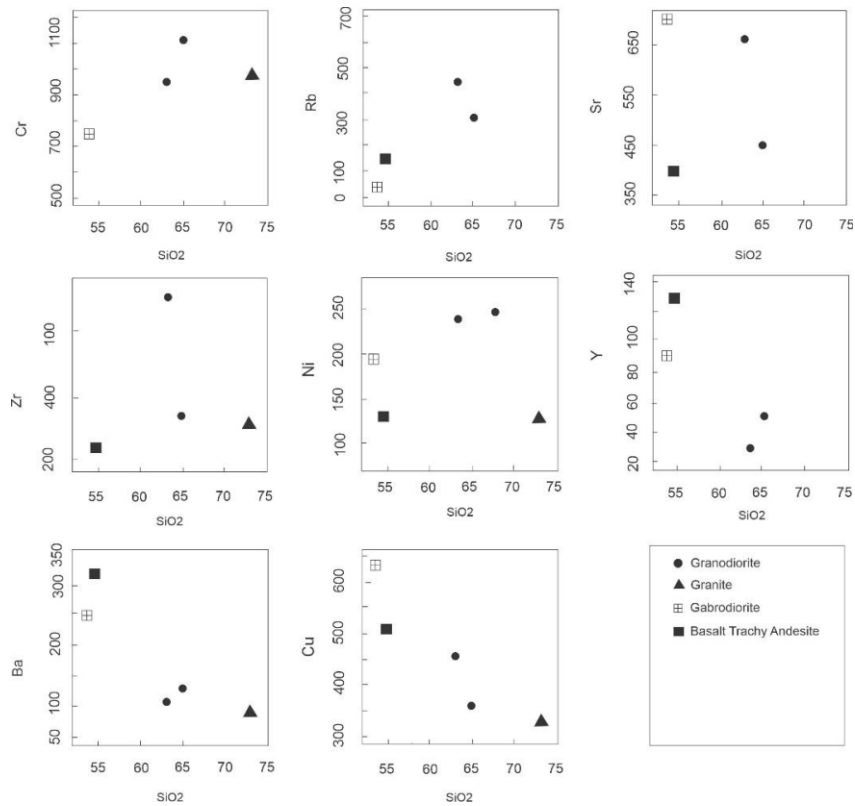


Fig. 15. Harker type variation diagram for trace elements of the rocks for the study area, see text for discussion.

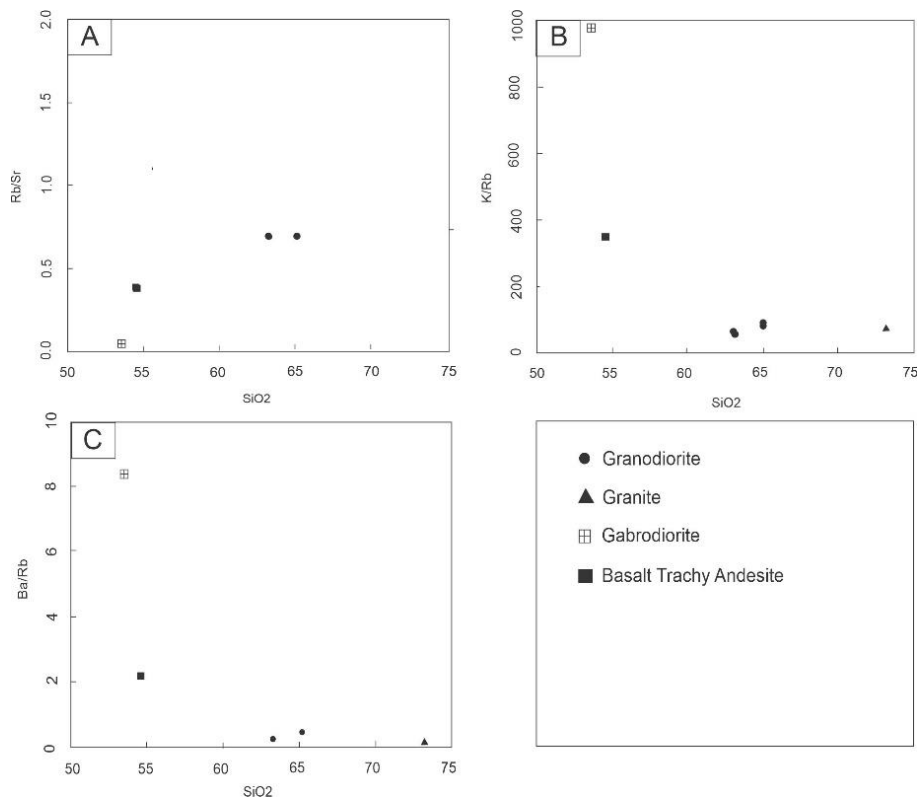


Fig. 16. shows elemental ratio of a) Rb/Sr, b) K/Rb, and c) Ba/Rb vs SiO₂, see text for discussion.

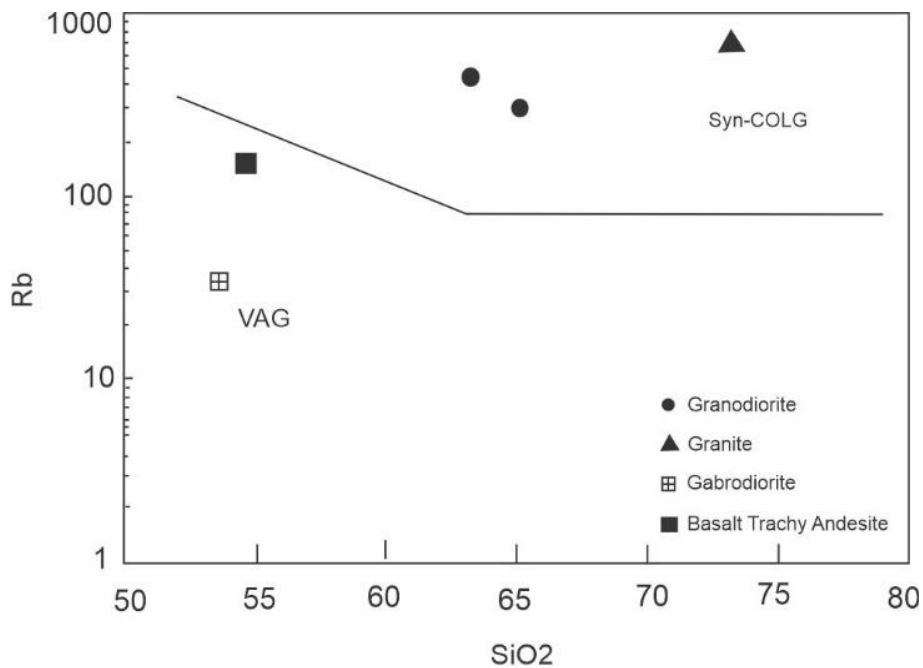


Fig. 15. Tectonic discrimination diagram SiO₂ vs Rb (Pearce et al., 1984) in which the granodiorite and granite show syncollision environment and gabbroic-diorite and basalt trachy andesite show volcanic arc environment.

5 Conclusion

This study presents the petrographic and geochemical investigation of the magmatic and volcanic intrusions exposed in Gilgit Metamorphic complex of the northern Kohistan Island Arc which were not previously studied. The SiO_2 and $\text{Na}_2\text{O}+\text{K}_2\text{O}$ values of the studied samples from these intrusions are in range of 53.60 to 73.19 wt.% and 4.55 to 9.13 wt.%, respectively. Geochemically, the rocks were recognized as granite, granodiorite, and gabbroic-diorite and basalt trachy andesite based on TAS diagrams for plutonic and volcanic rocks. The values of A/NK and A/CNK are in the range of 1.32 to 3.14 wt.% and 0.67 to 1.50 wt. %, respectively indicating calc-alkaline metaluminous magma series except granite rock which is peraluminous. The rocks show a calc-alkaline trend in the AFM diagram. In tectonic discrimination diagram the granite and granodiorite fall in syn-collisional field and the gabbroic diorite and basalt trachy andesite show volcanic arc environment. The Gabbro diorite and basalt trachy andesites have low silica content and are rich in Fe_2O_3 and MgO with low concentration of LILE elements. On the basis of geochemical and petrographical analyses the gabbro-diorite and basalt trachy andesite is primitive magma (less evolved) and intermediate in nature. Beside this, both granite and granodiorite show magma evolution with time. In addition, our study concludes that the upper mantle was the source for magmatism and the magmatism was more acidic with time forming acidic rocks.

Authors Contribution

Masroor Alam devised the theme, main concept, and structure of the manuscript. Hasnain Ali and Iqtidar Hussain contributed sampling, analysis and write up of the draft. Zahid helped in the discussion part. Muhammad Azam was involved in assistance in preparation of illustration and plates of figures. Sher Sultan Baig participated in providing relevant literature. Dr. Javed Akhtar Qureshi helped in English language correction while Hawas Khan contributed to the maps.

Acknowledgment

We are highly indebted to Prof. Dr. M. Asif Khan (Ex-Director, National Centre of Excellence in Geology, University of Peshawar) for his support in XRF and petrographic studies.

Conflict of Interest

There is no conflict of interest.

References

- Ali, A., Ahmad, S., Ahmad, S., Khan, M.A., M., Khan, M.I., and Rehman, G., 2021. Tectonic Framework of Northern Pakistan from Himalaya to Karakoram. Structural Geology and Tectonics Field Guidebook, 1, 367-412.
- Bard, J.P., Malusk, H., Matte, P., and Proust F.T., 1979. The Kohistan sequence; crust and mantle of an obducted island arc. Proceedings of International Conference on Geodynamics, Group 6, Meeting, Peshawar, Nov. 23-29, 1979: Special Issue of Geological Bulletin of University of Peshawar, 13, 87-94.
- Bignold, S.M., Treloar, P.J., and Petford, N., 2006. Changing sources of magma generation beneath intra-oceanic island arcs: An insight from the juvenile Kohistan Island Arc, Pakistan Himalaya. Chemical Geology, 233(1-2), 46-74.
- Blevin, P. L., 2004. Redox and Compositional Parameters for Interpreting the Granitoid Metallogeny of Eastern Australia: Implications for Gold-rich Ore Systems. Resource Geology, 54, 241-252.
- Cox, K.G., 2013. (Editor), The interpretation of igneous rocks. Springer Science & Business Media.
- Dhuime, B., Bosch, D., Garrido, C.J., and Bodinier, J.L., 2009. Geochemical Architecture of the Lower- to Middle-crustal Section of a Paleo-island Arc (Kohistan Complex, Jijal Kamila Area, Northern Pakistan): Implications for the Evolution of an Oceanic Subduction Zone. Journal of Petrology, 50, 531-569.
- Irvine, T.N., and Baragar, W.R.A., 1971. A guide to the chemical classification of common volcanic rocks. Canadian Journal of Earth Sciences, 8, 523-548.
- Jadoon, U.F., Huang, B., Zhao, Q., Shah, S.A., and Rahim, Y., 2021. Remagnetization of

- Jutal dykes in Gilgit area of the Kohistan Island Arc: Perspectives from the India–Asia collision. *Geophysical Journal International*, 226(1), pp.33-46.
- Jan, M.Q., 1970. Petrography of the upper part of Kohistan and southwestern Gilgit Agency along the Indus and Kandia rivers. *Geological Bulletin University of Peshawar*, 5, 27-48.
- Jan, M.Q., 1977. The Kohistan basic complex: A Summary based on recent petrological research. *Geological Bulletin University of Peshawar*, 9-10, 36-42.
- Jan, M.Q., 1979. Petrography of amphibolite of Swat and Kohistan. *Geological Bulletin Peshawar University*, 11, 51-64.
- Jung, S., and Hoernes, S., 2000. The major- and trace-element and isotope (Sr, Nd, O) geochemistry of Cenozoic alkaline rift-type volcanic rocks from the Rhön area (central Germany): petrology, mantle source characteristics and implications for asthenosphere–lithosphere interactions. *Journal of Volcanology and Geothermal Research*, 99, 27–53.
- Khan, T., 1994. Geology of a part of the Kohistan terranes between Gilgit and Chilas north Pakistan. *Geological Bulletin University of Peshawar*, 27, 99-112.
- Le Bas, M.J., Le Maitre, R.W., Streckeisen, A., and Zanettin, B., 1986. A chemical classification of volcanic rocks based on the total alkali-silica diagram. *Journal of Petrology*, 27(3), 745-750.
<https://doi.org/10.1093/petrology/27.3.745>
- Lee, J.I., 1997. Trace and rare earth element geochemistry of granitic rocks, southern part of the Kyongsang Basin. *Korean Geoscience Journal*, 1, 167-178.
- Patterson, M.G., and Windley, B.F., 1985. Rb-Sr dating of the Kohistan arc batholith in the trans Himalaya of north Pakistan and tectonic implications. *Earth and Planetary Science Letters*, 74, 45-57.
- Pearce J.A., Harris N.B.W., and Tindle, A.G., 1984. Trace Element Discrimination Diagrams for the Tectonic Interpretation of Granitic Rocks. *Journal of Petrology*, 25(4), 956-983.
- Petterson, M.G., 2010. A Review of the geology and tectonics of the Kohistan Island Arc, north Pakistan. *The Geological Society of London*, 338, 287–327.
- Pudsey, C.J., Coward, M.P., Luff, I.W., Shackleton, R.M., Windley, B.F., and Jan, M.Q., 1985. Collision zone between the Kohistan Arc and the Asian plate in NW Pakistan. *Earth and Environmental Science Transactions of the Royal Society of Edinburgh*, 76(4), 463-79.
- Pudsey, C.J., 1986. The Northern Suture, Pakistan: margin of a Cretaceous island arc. *Geological Magazine*, 123, 405–423.
- Shah, M. T., and Shervais, J.W., 1999. The Dir-Utror metavolcanic sequence, Kohistan Arc terrane, northern Pakistan. *Journal of Asian Earth Sciences*, 17(4), 459-475.
- Shand S.J., 1943. *The Eruptive Rocks*, 2nd Ed. John Wiley and Sons, New York, pp 1–444
- Sharma, K.K., 1991. Geology and geodynamic evolution of the Himalayan collision zone: a synthesis. *Physics and Chemistry of the Earth*, 18, 431–439. doi:10.1016/0079-1946(91)90013-6
- Tahirkheli, R.A.K., and Jan, M.Q., 1979. Geology of Kohistan, Karakoram, Himalaya, northern Pakistan. *Geological Bulletin of University of Peshawar*, 11, 1-187.
- Ugbe, F.C., Adiola, U.P., and Ebebare, U.C., 2016. Major and trace element geochemistry of granites in Kogi, Kogi State, Nigeria. *Research Journal of Environmental and Earth Sciences*, 8(1), 8-12.
- Ullah, Z., Khan, A., Faisal, S., Zafar, T., Li, H., and Farhan, M., 2022. Petrogenesis of peridotites in the Dargai Complex ophiolite, Indus Suture Zone, Northern Pakistan: Implications for two stages of melting, depletion, and enrichment of the Neo-Tethyan mantle. *Lithos*, 426, 106798.
- Ullah, Z., Li, H., Khan, A., Faisal, S., Dilek, Y., Förster, M.W., Farhan, M., Ashraf, U., Khattak, S.A., Rehman, G., and Hussain, S.A., 2023. Mineralogy and PGE geochemistry of chromitites and peridotites of the sapat complex in the indus suture zone, northern Pakistan: implications for magmatic processes in the supra-subduction zone. *International Geology Review*, 65(10), 1719-1744.
- Ullah, Z., Shah, M.T., Siddiqui, R.H., Lian, D.Y., and Khan, A., 2020. Petrochemistry of high-Cr and high-Al chromitites occurrences of dargai complex along indus

suture zone, northern Pakistan. *Episodes Journal of International Geoscience*, 43(2), 689-709.

Zafar, T., Leng, C.B., Mahar, M.A., Alam, M., Zhang, X.C., Chen, W.T., Rehman, H.U., and Rehman, S.U., 2020. Petrogenesis, platinum-group element geochemistry and geodynamic evolution of the Cretaceous Chilas gabbros, Kohistan Island arc, NE Pakistan. *Lithos*, 372, 105691.

Zhang, J., Wang, R., Hong, J., Tang, M., Zhu,

D.C., 2021. Nb-Ta systematics of Kohistan and Gangdese arc lower crust: Implications for continental crust formation. *Ore Geology Reviews*, 1 (133), 104131.

Searle, P.A., Molinski, T.F., Brzezinski, L.J., and Leahy, J.W., 1996. Absolute configuration of phorboxazoles A and B from the marine sponge *Phorbas* sp. 1. Macrolide and hemiketal rings. *Journal of the American Chemical Society*, 118(39), 9422-9423.